

# Calibrating Lévy Process from Observations Based on Neural Networks and Automatic Differentiation with Convergence Proofs<sup>☆</sup>

Kailai Xu<sup>a</sup>, Eric Darve<sup>b</sup>

<sup>a</sup>*Institute for Computational and Mathematical Engineering, Stanford University, Stanford, CA, 94305*

<sup>b</sup>*Mechanical Engineering, Stanford University, Stanford, CA, 94305*

---

## Abstract

The Lévy process has been widely applied to mathematical finance, quantum mechanics, peridynamics, turbulence flow, hydrodynamics and so on. However, calibrating the nonparametric multivariate distribution derived from the Lévy process from observations is a very challenging problem due to the lack of explicit distribution functions. In this paper, we propose a novel algorithm based on neural networks and automatic differentiation for solving this problem. We use neural networks to approximate the nonparametric part and discretize the characteristic exponents using accuracy numerical quadratures. Then we use automatic differentiation to compute gradients and minimize the mismatch between empirical and exact characteristic exponents using first-order optimization approaches. Another distinctive contribution of our work is that we made an effort to investigate the approximation ability of neural networks and the convergence behavior of algorithms. We derived the estimated number of neurons for a two-layer neural network. To achieve an accuracy of  $\varepsilon$  with the input dimension  $d$ , it is sufficient to build  $\mathcal{O}\left(\left(\frac{d}{\varepsilon}\right)^2\right)$  and  $\mathcal{O}\left(\frac{d}{\varepsilon}\right)$  for the first and second layers. The numbers are polynomial in the input dimension compared to the exponential  $\mathcal{O}\left(\varepsilon^{-d}\right)$  for one layer and therefore motivate the use of multilayer neural network. We also give the convergence proof of the neural network concerning the training samples under mild assumptions and show that the RMSE decreases linearly in the number of training data in the consistency error dominancy region for the 2D problem. It is the first-ever convergence analysis for such an algorithm in literature to our best knowledge. Finally, we apply the algorithms to the stock markets and reveal some interesting patterns in the pairwise  $\alpha$  index.

---

## 1. Introduction

The Lévy process generalizes the Gaussian process by allowing the jump diffusion. The probability density distribution (PDF) of such a process  $\{X_t\}_{t \geq 0}$ ,  $X_0 = \mathbf{x}$ , at  $t = t_1$  usually

---

<sup>☆</sup>The first author thanks the Stanford Graduate Fellowship in Science & Engineering and the 2018 Schlumberger Innovation Fellowship for the financial support.

*Email addresses:* [kailaix@stanford.edu](mailto:kailaix@stanford.edu) (Kailai Xu), [darve@stanford.edu](mailto:darve@stanford.edu) (Eric Darve)

has some desirable properties such as heavy tails, skewness and excess kurtosis that can improve modeling in many applications. The generator of the Lévy process can be written as [1]

$$\mathcal{A}f(\mathbf{x}) = \langle \xi, \nabla f(\mathbf{x}) \rangle + \frac{1}{2} \nabla \cdot A \nabla f(\mathbf{x}) + \int_{\mathbb{R}^d \setminus \{0\}} [f(\mathbf{x} + \mathbf{y}) - f(\mathbf{x}) - \nabla f(\mathbf{x}) \cdot \mathbf{y} \mathbf{1}_{|\mathbf{y}| \leq 1}] \nu(\mathbf{y}) d\mathbf{y} \quad (1)$$

where  $\int_{\mathbb{R}^d \setminus \{0\}} (1 \wedge |\mathbf{x}|^2) \nu(\mathbf{x}) d\mathbf{x} < \infty$ ,  $1 \wedge |\mathbf{x}|^2 = \min\{1, |\mathbf{x}|^2\}$ ,  $\xi \in \mathbb{R}^d$ ,  $A$  is a semidefinite positive matrix.

For example, in mathematical finance, the exponential Lévy models are usually used to model asset price [2]. There are a family of such models, and we briefly list them here

- The *Merton's model* [3] is one of the first jump processes in financial modeling, where one adds Gaussian jumps to the log-price

$$S_t = S_0 e^{rt+X_t}, \quad X_t = \gamma t + \sigma W_t + \sum_{i=1}^{N_t} Y_i, \quad Y_i \sim \mathcal{N}(\mu, \delta^2) \quad (2)$$

It allows underlying stock returns to be discontinuous.

- The *Kou model* [4] has the jump sizes are modeled with the Lévy density function of the form

$$\nu(dx) = [p \lambda_+ e^{-\lambda_+ x} \mathbf{1}_{x>0} + (1-p) \lambda_- e^{-\lambda_- |x|} \mathbf{1}_{x<0}] dx \quad (3)$$

- The *variance gamma process* [5] has the Lévy measure of the form

$$\nu(x) = \frac{c_-}{|x|} e^{-\lambda_- |x|} \mathbf{1}_{x<0} + \frac{c_+}{x} e^{-\lambda_+ x} \mathbf{1}_{x>0} \quad (4)$$

- The *CGMY model* [6] directly specifies the Lévy density

$$\nu(x) = \frac{c_-}{|x|^{1+\alpha_-}} e^{-\lambda_- |x|} \mathbf{1}_{x<0} + \frac{c_+}{x^{1+\alpha_+}} e^{-\lambda_+ x} \mathbf{1}_{x>0} \quad (5)$$

Besides mathematical finance, the Lévy process also finds its applications in quantum mechanics where the Lévy process is considered as the underlying stochastic process powering the random fluctuations [7–10]. For any distribution with power-law decay  $\frac{1}{|x|^{1+\alpha}}$ ,  $0 < \alpha < 1$  the generalized central limit theorem guarantee that their sum scaled by  $\frac{1}{n^{1/\alpha}}$  converge to the  $\alpha$ -stable distribution. If the variance is finite, i.e.,  $\alpha \geq 2$ , then the central limit theorem holds, where their sum scaled by  $\frac{1}{n^{1/2}}$ , properly centered, and identically distributed, converge to the Gaussian distribution. It leads to the fractional Schrödinger equation

$$i\hbar \partial_t \psi(x, t) = D_\alpha (-\hbar^2 \Delta)^{\alpha/2} \psi(x, t) \quad (6)$$

where  $(-\hbar^2 \Delta)^{\alpha/2}$  is the fractional Laplacian which can be defined through

$$(-\hbar^2 \Delta)^{\alpha/2} \psi(x, t) = \frac{1}{(2\pi\hbar)^3} \int |\xi|^\alpha \hat{\psi}(\xi, t) \exp(i(\xi, x)/\hbar) d\xi \quad (7)$$

More generally, other Lévy measures can be used to develop quantum mechanics. The more general Schrödinger equation reads

$$i\hbar\partial_t\psi(x, t) = -\frac{\hbar^2}{2m}\partial_x^2\psi(x, t) - \hbar\int_{\mathbb{R}}[\psi(x+y, t) - \psi(x, t)]\nu(y)dy \quad (8)$$

Some examples of the Lévy-Schrödinger equations are

- Relativistic.

$$i\hbar\partial_t\psi(x, t) = \sqrt{m^2c^4 - c^2\hbar^2\partial_x^2}\psi(x, t) \quad (9)$$

- Variance-Gamma laws

$$i\hbar\partial_t\psi(x, t) = -\frac{\lambda\hbar}{\tau}\int_{\mathbb{R}}\frac{\psi(x+y, t) - \psi(x, t)}{|y|}e^{-|y|/\hbar}dy \quad (10)$$

However, since there is usually no closed form of the PDF, the calibration of the parameters are very challenging. It is particularly challenging if  $\nu$  is given by an arbitrary function, which form a infinite dimensional space [11]. For example, the standard maximum likelihood methods are not directly application due to the lack of explicit PDFs. However, a significant advantage of the Lévy models is their mathematical tractability: the characteristic functions of the distributions take an explicit form thanks to the Lévy–Khintchine representation theorem. The calibration problem is already challenging in the univariate case. Here in this paper, we consider a more general and challenging problem: the multivariate nonparametric problems. That is, there may be unknown functions instead of parameters in the Lévy density function.

Based on whether the Lévy density has a singularity, we consider two kinds of problems with different algorithms

- The Lévy density function has a singularity. eqs. (4), (5), (7) and (10) are such examples. In this case, we use an explicit formula for the singularity part. We give an example of calibrating multivariate stable distribution in section 2.
- The Lévy density function is continuous. eqs. (2) and (3) are such examples. We give an example of calibrating the distribution from the Lévy process in section 3.

Machine learning methods have proved very useful in solving data-driven problems. Recently deep learning has been successfully used to address a variety of applications [12–14]. Two of the critical ingredients for its success are the non-linear neural networks [15], which are used for approximating a high dimensional complicated function; another is the automatic differentiation [16], which is rebranded as “back-propagation” [17] in deep learning.

*Multilayer neural networks* have been around for a long time [18–20]. However, a systematic mathematical theory characterizing the properties of the multilayer neural networks is still missing. In this paper, we make an effort to motivate multilayer neural networks over a single layer neural network regarding the number of neurons required for the hidden

sizes to achieve a certain accuracy with the sigmoid activation function. In particular, we proved that if a single layer and sigmoid activation functions are used, the estimated number of neurons grows exponentially with the input dimension. However, if a two-layer neural network is used, the estimated numbers of neurons for the first and second layer increase quadratically and linearly respectively with the input dimension.

*Automatic differentiation* (AD) is a technique for computing the gradients of any complicated function of its inputs and parameters [16]. There are mainly two ways for AD: forward mode and backward mode. The power of AD is that it combines the accuracy and efficiency of symbolic differentiation and computation graph derived from the chain rule. It effectively eliminates “human” coding errors. It has already been widely applied to machine learning, sensitivity analysis in engineering, optimization, etc. In this paper, all the gradients are computed using AD, and therefore the implementation is straightforward and direct.

In this paper, we consider the following problem: given one or several sample paths  $\{X_{n\Delta t}\}_{n=1}^N$  from the Lévy process, we want to estimate the parameters  $\xi$ ,  $A$  as well as  $\nu(\mathbf{y})$  in eq. (1). The models are allowed to be parametric or nonparametric. We apply the characteristic function matching approach [21], where we first compute the empirical characteristic function (ECF) from the data. We then sample from ECF, and for every tuple  $(\xi, A, \nu)$ ; we can compute a fidelity function from the sample values and inferred values from the tuple. A first-order method is used to minimize the fidelity function by varying the tuple. Note here AD is applied and therefore we do not have to code the gradients of the fidelity function.

We also investigate the “convergence” of the neural network as we increase the training data. We give a proof of the convergence based on mild assumptions on the data and the optimization. To the best knowledge of the authors, this is the first time such analysis is given in the literature. We proved that for the problem in section 3, the root mean square error decreases linearly in the number of sampling points. The convergence proof and the convergence rate are closely related to that of the finite element method/finite difference method.

We summarize our contributions here

- Proposed a framework for calibrating nonparametric Lévy processes based on neural networks and automatic differentiation.
- Derived an estimated number of neurons for two-layer neural network with sigmoid activation functions.
- Derived an error bound and calculated the convergence rate for the RMSE of the fidelity function.
- Applied the proposed algorithm to the stock markets and revealed interesting patterns in the pairwise  $\alpha$  index.

For convenience, we list the symbols we used in the paper in table 1. The codes for this project are available at the following url

<https://github.com/kailaix/levyml>

May 31, 2022

Noation	Description
$\nu$	Lévy density function
$N$	Number of points in the Lévy path
$n$	Number of sampling points in the frequency domain
$n_q$	$n_q^2$ is the number of quadrature points
$n_l$	Number of layers
$n_h$	Number of hidden layers
$a, b, c$	Coefficients for the diffusion term
RMSE	Root mean square error on the collocation points for testing
$\lesssim$	$f(x) \lesssim g(x)$ indicates there exists $C > 0$ , independent of $x$ , such that $f(x) \leq Cg(x)$

Table 1: Notations

## 2. Multivariate stable distributions

We consider the stable random vector  $\mathbf{X} = (X_1, X_2, \dots, X_d) \in \mathbb{R}^d$  whose characteristic function is

$$\varphi(\xi) = \mathbb{E}(e^{i\langle \mathbf{X}, \xi \rangle}) = \exp(I(\xi)) \quad (11)$$

where the exponent function  $I(\xi)$  is given by [22]

$$I(\xi) = - \int_{S^d} \psi(\langle \xi, \mathbf{s} \rangle) \Gamma(d\mathbf{s}) + i\langle \xi, \mu \rangle \quad (12)$$

Here  $S^d$  is the unit sphere in  $\mathbb{R}^d$  and  $\langle \cdot, \cdot \rangle$  denotes inner product,  $\Gamma$  is called the finite spectral measure on  $S^d$ ,  $\mu = (\mu_1, \mu_2, \dots, \mu_d) \in \mathbb{R}^d$  is the location vector, and

$$\psi(u) = \begin{cases} |u|^\alpha (1 - i\text{sign}(u) \tan \frac{\pi\alpha}{2}) & \alpha \neq 1 \\ |u| (1 + i\frac{2}{\pi}\text{sign}(u) \log |u|) & \alpha = 1 \end{cases} \quad (13)$$

here  $\alpha \in (0, 2]$  is the fractional index, which is related to the tail thickness.

Given an i.i.d. sample  $\mathbf{X}_1, \mathbf{X}_2, \dots, \mathbf{X}_n$  drawn from this distribution, our task is to estimate  $\alpha$  as well as the finite spectral measure. There has been vast literature investigating the univariate and multivariate case. In the univariate case,  $\Gamma$  can be characterized by two parameters  $\beta, \sigma$ ; the most popular parametrization of the characteristic exponent is [23]

$$I(\xi) = \begin{cases} -\sigma^\alpha |\xi|^\alpha (1 - i\beta\text{sign}(\xi) \tan \frac{\pi\alpha}{2}) + i\mu\xi & \alpha \neq 1 \\ -\sigma|t| (1 + i\beta\text{sign}(t) \frac{2}{\pi} \log |t|) + i\mu t & \alpha = 1 \end{cases} \quad (14)$$

We usually denote the distribution by  $X \sim S_\alpha(\sigma, \beta, \mu)$ . Even though the characteristic function has an explicit and simple formula, the closed form formulas for most stable densities and distribution functions are lacking. To evaluate the distribution function, either fast Fourier transform [24] or direct numerical integration method [25] has to be utilized.

The complexity of the density function is an obstacle to the popular maximum likelihood estimation. Besides, since stable distributions do not necessarily have higher order moments, the method of moments do not apply here [26]. This difficulty already exists in the univariate case. For the multivariate case, since we have no parametrized model for  $\Gamma$ , the calibration of the stable distribution is much more challenging.

There are some efforts in literature. In [22], the author approximated the finite spectral measure with a finite number of point masses, i.e.,

$$\Gamma(\cdot) = \sum_{j=1}^n \gamma_j \delta_{\mathbf{s}_j}(\cdot) \quad (15)$$

where  $\gamma_j$ 's are the weights, and  $\delta_{\mathbf{s}_j}$ 's are point masses at the points  $\mathbf{s}_j \in S^d$ . Under such a discrete spectral measure, the characteristic exponent becomes parametrized

$$I(\xi) = - \sum_{j=1}^n \psi_\alpha(\langle \xi, \mathbf{s}_j \rangle) \gamma_j + i \langle \xi, \mu \rangle \quad (16)$$

[26] adopts this idea and considers the generalized empirical likelihood (GEL) method for estimating the parameters of the multivariate stable distribution. In GEL, the empirical likelihood ratio function for a parameter  $\theta$  is defined as

$$L(\theta) = \max_{(p_1, p_2, \dots, p_n)} \left\{ \prod_{j=1}^n np_j \left| \sum_{j=1}^n p_j g(X_j, \theta) = 0, \sum_{j=1}^n p_j = 1, p_j \geq 0 \right. \right\} \quad (17)$$

here  $g$  is a function that estimates the mismatch between model  $\theta$  and data.

In this paper, instead of firstly parametrizing the finite spectral measure, we represent  $\Gamma$  directly using a neural network.

Suppose the multilayer neural network approximation to  $\Gamma(\mathbf{s})$  is  $\Gamma_{\mathbf{w}}(\mathbf{s})$ , where  $\mathbf{w}$  is the weight parameter. One distinguishing feature of a multilayer neural network approximation is that they are dense in  $C(S^d)$  [27], and also, the gradients with respect to  $\mathbf{w}$ ,  $\nabla_{\mathbf{w}} \Gamma_{\mathbf{w}}$  can be computed exactly. Suppose that  $\{\mathbf{X}_j\}$  is an i.i.d. sequence from the same distribution, using the law of large numbers, if  $n$  is sufficiently large, we can approximate the characteristic function by the empirical characteristic function

$$\varphi_E(\xi) = \frac{1}{N} \sum_{i=1}^N \exp(i \langle \xi, \mathbf{X}_i \rangle) \quad (18)$$

and the corresponding empirical characteristic exponent

$$I_E(\xi) = \log(\varphi_E(\xi)) \quad (19)$$

Since we have

$$I(\xi) = - \int_{S^d} |\langle \xi, \mathbf{s} \rangle|^\alpha \Gamma(\mathbf{s}) d\mathbf{s} + i \langle \xi, \mu \rangle + i \tilde{\psi}(\alpha, \Gamma, \xi) \quad (20)$$

here

$$\tilde{\psi}(\alpha, \Gamma, \xi) = \begin{cases} - \int_{S^d} \text{sign}(\langle \xi, \mathbf{s} \rangle) \tan \frac{\pi \alpha}{2} \Gamma(\mathbf{s}) d\mathbf{s} & \alpha \neq 1 \\ - \frac{2}{\pi} \int_{S^d} \text{sign}(\langle \xi, \mathbf{s} \rangle) \log |\langle \xi, \mathbf{s} \rangle| \Gamma(\mathbf{s}) d\mathbf{s} & \alpha = 1 \end{cases} \quad (21)$$

We can then construct a loss function aiming at matching the real part of the model characteristic exponent and the empirical characteristic exponent

$$R(\mathbf{w}, \alpha) = \frac{1}{n} \sum_{j=1}^n \left( - \int_{S^d} |\langle \xi_j, \mathbf{s} \rangle|^\alpha \Gamma_{\mathbf{w}}(\mathbf{s}) d\mathbf{s} - \Re I_E(\xi_j) \right)^2 \quad (22)$$

where  $\{\xi_j\}_{j=1}^N$  are  $N$  randomly sampled collocation points in the *frequency domain*. For the integral, since we cannot evaluate it analytically given the neural network  $\Gamma$ , we need to apply numerical quadratures. Here we apply a numerical quadrature for the sphere.

$$R(\mathbf{w}, \alpha) = \frac{1}{n} \sum_{j=1}^n \left( - \sum_{k=1}^{n_q} |\langle \xi_j, \mathbf{s}_k \rangle|^\alpha \Gamma_{\mathbf{w}}(\mathbf{s}_k) w_k - \Re I_E(\xi_j) \right)^2 \quad (23)$$

here  $\{\mathbf{s}_k\}$ ,  $\{w_k\}$  are numerical points and weights respectively.

By minimizing the loss function eq. (23) we obtained the estimators for  $\alpha$  and  $\Gamma$  (in terms of  $\mathbf{w}$ )

$$\hat{\alpha}, \hat{\mathbf{w}} = \arg \min_{\alpha, \mathbf{w}} R(\mathbf{w}, \alpha) \quad (24)$$

The next step is to calibrate the drift term  $i\langle \xi, \mu \rangle$ . We apply the least square methods to the imaginary part of the characteristic function

$$\mu = \arg \min_{\mu} \sum_{j=1}^N \left| \langle \xi_j, \mu \rangle + \tilde{\psi}(\hat{\alpha}, \Gamma_{\mathbf{w}}, \xi_j) - \Im I_E(\xi_j) \right|^2 \quad (25)$$

We have chosen to separate calibration real parts and imaginary parts sequentially for several practical considerations

- There is singularity in  $\tilde{\psi}$  with respect to  $\alpha$  near  $\alpha = 1$ . That will impede accurate numerical integration and optimization in the training phase. We avoid this problem by learning  $\alpha$  separately and then apply the robust least square methods.
- In some applications, the amplitude of the data spectrum instead of the phase is much more important. Here the exponential of the real part is exactly the amplitude while the imaginary part controls the phase. By the sequential calibrating approach, we can avoid the impact from the noise in the phase of the data.
- The goodness-of-fit for the least squares problem eq. (25) serves as a natural indicator of whether the multivariate stable distribution is a good model for the data provided.

In practice, it may be difficult to find the minimum for eq. (23), but a good local minimum may suffice for real applications.

### 3. Lévy Process with Continuous Lévy Density Functions

The multivariate stable distribution is a special case arising in the Lévy process models. We consider the Lévy process which is defined as follows [28]

**Definition 3.1.** A càdlàg (right continuous with left limits) real valued stochastic process  $\{\mathbf{X}_t\}_{t \geq 0}$  such that  $\mathbf{X}_0 = 0$  is called a Lévy process if it has stationary independent increments and is stochastically continuous.

The characteristic function of  $\mathbf{X}_t$  is given by the Lévy-Khintchine representation [29]

$$\mathbb{E}(\exp(i\xi \mathbf{X}_t)) = \exp \left( t \left( i \langle \xi, \mu \rangle - \frac{1}{2} \langle \xi, A\xi \rangle + \int_{\mathbb{R}^d \setminus \{0\}} (e^{i\langle \xi, \mathbf{x} \rangle} - 1 - i \langle \xi, \mathbf{x} \rangle \mathbf{1}_{|\mathbf{x}| \leq 1}) \nu(\mathbf{x}) d\mathbf{x} \right) \right) \quad (26)$$

where  $\mu \in \mathbb{R}^d$ ,  $Q$  is a positive-definite matrix of size  $d \times d$  and  $\nu(\mathbf{x})$  is called the Lévy measure. It is a positive measure that satisfies

$$\int_{\mathbb{R}^d \setminus \{0\}} (1 \wedge |\mathbf{x}|^2) \nu(\mathbf{x}) d\mathbf{x} < \infty \quad (27)$$

here  $1 \wedge |\mathbf{x}|^2 = \min\{1, |\mathbf{x}|^2\}$ .

The Lévy process can be decomposed into two parts: the first part is the Brownian motion, which is continuous; the second part is an infinite sum of the Poisson process. We allow  $\nu(\mathbf{x})$  to be an infinite measure as long as it satisfies eq. (27).

In this section we consider calibrating the model eq. (26) with unknowns  $\mu$ ,  $A$  and  $\nu(\mathbf{x})$ . Suppose the observations are i.i.d. samples from the same distribution as  $\mathbf{X}_{\Delta t}$ ; and without loss of generosity,  $\Delta t = 1$ . The samples are denoted as  $\{X_j\}_{j=1}^N$  with a little abuse of notations.

We assume that  $\nu(\mathbf{x})$  is continuous so that  $\nu(\mathbf{x}) < \infty$ . We can absorb the term  $-i \int_{\mathbb{R}^d \setminus \{0\}} \langle \xi, \mathbf{x} \rangle \mathbf{1}_{|\mathbf{x}| \leq 1} \nu(\mathbf{x}) d\mathbf{x}$  into the drift term. Thus the characteristic exponent for the data is

$$I(\xi) = i \langle \xi, \mu \rangle - \frac{1}{2} \langle \xi, A\xi \rangle + \int_{\mathbb{R}^d \setminus \{0\}} (e^{i\langle \xi, \mathbf{x} \rangle} - 1) \nu(\mathbf{x}) d\mathbf{x} \quad (28)$$

Likewise, we can compute the empirical characteristic exponent as in eqs. (18) and (19).

Now we consider using a neural network approximation  $\nu_{\mathbf{w}}(\mathbf{x})$  to the Lévy measure  $\nu(\mathbf{x})$ . Let  $\{\mathbf{x}_j\}_{j=1}^{n_q^2}$  and  $\{w_j\}_{j=1}^{n_q^2}$  be the numerical quadrature points and weights on the square domain  $[-L, L]^2$ , where  $L$  depends on specific problems (See Section B).

We construct the loss function to minimize by matching the real part of the real part of the approximated characteristic exponent and the empirical ones

$$R(\mathbf{w}, A) = \sum_{j=1}^N \left( -\frac{1}{2} \langle \xi_j, A\xi_j \rangle + \sum_{k=1}^{n_q^2} (\cos \langle \xi_j, \mathbf{x}_k \rangle - 1) \nu_{\mathbf{w}}(\mathbf{x}_k) w_k - \Re I_E(\xi_j) \right)^2 \quad (29)$$

By minimizing eq. (29), we obtain the estimators  $\hat{\mathbf{w}}$  and  $\hat{A}$

$$\hat{\mathbf{w}}, \hat{A} = \arg \min_{\mathbf{w}, A} R(\mathbf{w}, A) \quad (30)$$

To estimate  $\mu$ , we again use least square methods

$$\mu = \arg \min_{\mu} \sum_{j=1}^N \left| \langle \xi_j, \mu \rangle + \sum_{k=1}^{n_q^2} \sin \langle \xi_j, \mathbf{x}_k \rangle \nu_{\hat{\mathbf{w}}}(\mathbf{x}_k) w_k - \Im I_E(\xi_j) \right|^2 \quad (31)$$

Again, the goodness-of-fit of eq. (31) can serve as a good indicator whether the Lévy model is proper for the observed data.

## 4. Convergence Analysis

### 4.1. Approximation by Neural Networks

The approximation degree for one layer neural network is well understood in literature. One such result is [30]

**Theorem 1.** Let  $1 \leq d' \leq d$ ,  $r \geq 1$ ,  $d \geq 1$  be integers,  $1 \leq p \leq \infty$ ,  $\varphi : \mathbb{R}^{d'} \rightarrow \mathbb{R}$  be infinitely many times continuously differentiable in some open sphere in  $\mathbb{R}^{d'}$ . We further assume that there exists  $\mathbf{b}$  in this sphere such that

$$\mathbf{D}^{\mathbf{k}} \varphi(\mathbf{b}) \neq 0, \quad \mathbf{k} \in \mathbb{Z}^{d'}, \mathbf{k} \geq \mathbf{0} \quad (32)$$

Then there exist  $d' \times d$  matrices  $\{A_j\}_1^n$  with the following property. For any  $f \in W_{r,d}^p$ , there exist coefficients  $a_j(f)$  such that

$$\|f - \sum_{j=1}^n a_j(f) \varphi(A_j(\cdot) + \mathbf{b})\|_p \leq cn^{-r/d} \|f\|_{W_{r,d}^p} \quad (33)$$

Here

$$\|f\|_{W_{r,d}^p} = \sum_{0 \leq |\mathbf{k}| \leq r} \|D^{\mathbf{k}} f\|_p \quad (34)$$

with multi-integer  $\mathbf{k} = (k_1, k_2, \dots, k_s)$

For example, if  $d' = 1$ , and  $\varphi = \sigma$  is the sigmoid function, then  $\varphi$  satisfies the condition in the theorem. If  $f \in W_{1,d}^p$  (and therefore  $r = 1$ ), we obtain a neural network with one hidden layer (hidden size equals  $n$ ). To achieve a predetermined error  $\varepsilon > 0$ , we need

$$n^{-1/d} = \mathcal{O}(\varepsilon) \Rightarrow n = \mathcal{O}(\varepsilon^{-d}) \quad (35)$$

This indicates that one layer neural network suffers from the curse of dimensionalities – the number of required hidden layers grows exponentially with the input dimension  $d$ .

One possible way to overcome this difficulty is to consider multilayer neural network. We will now consider this possibility.

In the late 1950s, Kolmogorov proved in a series of papers the Kolmogorov Superposition Theorem that answers (in the negative) Hilbert's 13th problem (see section A). It is a theorem about representing instead of approximating and quite deep. It says that for a continuous function defined on  $[0, 1]^d$ , given appropriate activation function, a neural network with hidden sizes  $\mathcal{O}(d)$  will be able to represent the function *exactly*.

**Theorem 2** (Kolmogorov Superposition Theorem [31]). There exist  $d$  constants  $\lambda_j > 0$ ,  $j = 1, 2, \dots, d$ ,  $\sum_{j=1}^d \lambda_j \leq 1$  and  $2n + 1$  strictly increasing continuous function  $\phi_i$ ,  $i = 1, 2, \dots, 2d + 1$ , which map  $[0, 1]$  to itself, such that every continuous function  $f$  of  $d$  variables on  $[0, 1]^d$  can be represented in the form

$$f(x_1, \dots, x_d) = \sum_{i=1}^{2d+1} g \left( \sum_{j=1}^d \lambda_j \phi_i(x_j) \right) \quad (36)$$

for some  $g \in C[0, 1]$  depending on  $f$ .

Based on the above result, Maiorov and Pinkus [32] proved that if the fixed number of units in the hidden layers are  $6d + 3$  and  $3d$ , the two-layer neural networks can approximate any function to arbitrary precision.

**Theorem 3.** There exists an activation function  $\sigma$  which is analytical, strictly increasing and sigmoidal and has the following property: for any  $f \in C[0, 1]^d$  and  $\varepsilon > 0$ , there exist constants  $d_i$ ,  $c_{ij}$ ,  $\theta_{ij}$ ,  $\gamma_i$  and vectors  $\mathbf{w}^{ij} \in \mathbb{R}^d$  for which

$$\left| f(\mathbf{x}) - \sum_{i=1}^{6d+3} d_i \sigma \left( \sum_{j=1}^{3d} c_{ij} \sigma(\mathbf{w}^{ij} \cdot \mathbf{x} - \theta_{ij}) - \gamma_i \right) \right| < \varepsilon$$

for all  $\mathbf{x} = (x_1, \dots, x_d) \in [0, 1]^d$ .

Theorems 2 and 3 only implies that the approximation ability of two-layer neural network for appropriate activation functions. These activation functions can be quite pathological to achieve the desired accuracy. It is unclear if the activation functions used in practice, such as sigmoid function, suffice for accurate approximation.

For any  $f \in C[0, 1]^d$ , let the corresponding superposition decomposition be eq. (36). Consider the family of the functions  $f$  where the corresponding  $g \in W_{1,1}^p$  and  $\phi_i(x) \in W_{1,1}^p$ , then by theorem 1, there exist constants  $w_{ri}$ ,  $a_{ri}$ ,  $b_{ri}$  and a constant  $C > 0$  independent of  $r$ , such that

$$\left| g(t) - \sum_{i=1}^r w_{ri} \sigma(a_{ri}t + b_{ri}) \right| \leq \frac{C \|g\|_{W_{1,1}^p}}{r} \quad (37)$$

We call the function family of  $f$  a *regular family* if  $w_{ri}$ ,  $a_{ri}$  are bounded independent of  $r$ , i.e., there exists a constant  $\tilde{C}$ , s.t.

$$|w_{ri}| \leq \tilde{C}, |a_{ri}| \leq \tilde{C} \quad i = 1, 2, \dots, r, \quad \forall r \quad (38)$$

**Remark 1.** The assumptions that  $g \in W_{1,1}^p$  and  $\phi_i(x) \in W_{1,1}^p$  are critical for our derivative for the error bound. Note that even strictly increasing continuous functions can be very pathological. An example is the the Cantor function  $\mathcal{D}(x)$ .  $\mathcal{D}(x)$  is a nondecreasing continuous function but does not have a weak derivative.  $x + \mathcal{D}(x)$  will then be a strictly increasing continuous function but has no weak derivatives. We want to avoid this kind of functions in this paper.

We now derive an explicit error bound for approximating a function in the regular family by a two-layer neural network with sigmoid functions as the activation functions.

**Theorem 4.** Let  $\sigma$  be the standard sigmoid function

$$\sigma(x) = \frac{1}{1 + e^{-x}} \quad (39)$$

then for any  $f$  in the regular family and  $\varepsilon > 0$ , there exists a two layer neural network with hidden units  $s = \mathcal{O}\left(\frac{d^2}{\varepsilon^2}\right)$  (the first layer) and  $r = \mathcal{O}\left(\frac{d}{\varepsilon}\right)$  (the second layer), and constants  $d_i, c_{ij}, \theta_{ij}, \gamma_i$  and vectors  $\mathbf{w}^{ij} \in \mathbb{R}^d$  for which

$$\left| f(\mathbf{x}) - \sum_{i=1}^r d_i \sigma \left( \sum_{j=1}^s c_{ij} \sigma(\mathbf{w}^{ij} \cdot \mathbf{x} - \theta_{ij}) - \gamma_i \right) \right| < \varepsilon \quad (40)$$

for all  $\mathbf{x} = (x_1, \dots, x_d) \in [0, 1]^d$ .

*Proof.* We apply the assumption eq. (37) to eq. (36) we have

$$\left| \sum_{i=1}^{2d+1} g \left( \sum_{j=1}^d \lambda_j \phi_i(x_j) \right) - \sum_{i=1}^{2d+1} \sum_{k=1}^r w_{rk} \sigma \left( a_{rk} \left( \sum_{j=1}^d \lambda_j \phi_i(x_j) \right) + b_{rk} \right) \right| \lesssim \sum_{i=1}^{2d+1} \frac{1}{r} \lesssim \frac{d}{r} \quad (41)$$

For any  $i = 1, 2, \dots, 2d+1$ , there exist coefficients  $w_l^i, a_l^i, b^i$  such that

$$\left| \phi_i(x_j) - \sum_{l=1}^s w_l^i \sigma(a_l^i x_j + b^i) \right| \lesssim \frac{1}{s}$$

Plug it into eq. (36) we have

Since

$$|\sigma'(x)| = |\sigma(x)(1 - \sigma(x))| \leq 1$$

we have

$$\begin{aligned} & \left| \sigma \left( a_{rk} \sum_{j=1}^d \lambda_j \phi_i(x_j) + b_{ri} \right) - \sigma \left( a_{rk} \sum_{j=1}^d \lambda_j \sum_{l=1}^s w_l^i \sigma(a_l^i x_j + b^i) + b_{ri} \right) \right| \\ & \leq |a_{rk}| \sum_{j=1}^d \lambda_j \left| \phi_i(x_j) - \sum_{l=1}^s w_l^i \sigma(a_l^i x_j + b^i) \right| \\ & \lesssim \frac{1}{s} \sum_{j=1}^d \lambda_j = \frac{1}{s} \end{aligned} \quad (42)$$

Plug eq. (42) into eq. (41) we have

$$\begin{aligned}
& \left| \sum_{i=1}^{2d+1} \sum_{k=1}^r w_{rk} \sigma \left( a_{rk} \left( \sum_{j=1}^d \lambda_j \phi_i(x_j) \right) + b_{rk} \right) \right. \\
& \quad \left. - \sum_{i=1}^{2d+1} \sum_{k=1}^r w_{rk} \sigma \left( a_{rk} \left( \sum_{j=1}^d \lambda_j \sigma \left( a_{rk} \sum_{j=1}^d \lambda_j \sum_{l=1}^s w_l^i \sigma(a_l^i x_j + b^i) + b_{ri} \right) \right) + b_{rk} \right) \right| \quad (43) \\
& \lesssim \sum_{i=1}^{2d+1} \sum_{k=1}^r |w_{rk}| \frac{1}{s} \lesssim \frac{dr}{s}
\end{aligned}$$

Thus we obtained

$$\left| f(\mathbf{x}) - \sum_{i=1}^{2d+1} \sum_{k=1}^r w_{rk} \sigma \left( a_{rk} \left( \sum_{j=1}^d \lambda_j \sigma \left( a_{rk} \sum_{j=1}^d \lambda_j \sum_{l=1}^s w_l^i \sigma(a_l^i x_j + b^i) + b_{ri} \right) \right) + b_{rk} \right) \right| \quad (44)$$

$$\leq \left| \sum_{i=1}^{2d+1} g \left( \sum_{j=1}^d \lambda_j \phi_i(x_j) \right) - \sum_{i=1}^{2d+1} \sum_{k=1}^r w_{rk} \sigma \left( a_{rk} \left( \sum_{j=1}^d \lambda_j \phi_i(x_j) \right) + b_{rk} \right) \right| \quad (45)$$

$$+ \left| \sum_{i=1}^{2d+1} \sum_{k=1}^r w_{rk} \sigma \left( a_{rk} \left( \sum_{j=1}^d \lambda_j \phi_i(x_j) \right) + b_{rk} \right) \right| \quad (46)$$

$$- \sum_{i=1}^{2d+1} \sum_{k=1}^r w_{rk} \sigma \left( a_{rk} \left( \sum_{j=1}^d \lambda_j \sigma \left( a_{rk} \sum_{j=1}^d \lambda_j \sum_{l=1}^s w_l^i \sigma(a_l^i x_j + b^i) + b_{ri} \right) \right) + b_{rk} \right) \quad (47)$$

$$\leq \frac{d}{r} + \frac{dr}{s} \quad (48)$$

To achieve error  $\varepsilon$  we let

$$\frac{d}{r} = \mathcal{O}(\varepsilon) \quad \frac{dr}{s} = \mathcal{O}(\varepsilon) \quad (49)$$

and we have

$$r = \mathcal{O} \left( \frac{d}{\varepsilon} \right) \quad s = \mathcal{O} \left( \frac{d^2}{\varepsilon^2} \right) \quad (50)$$

By regrouping and renaming the coefficients we obtain eq. (40). The result indicates the first layer has  $\mathcal{O} \left( \frac{d^2}{\varepsilon^2} \right)$  neurons and the second layer has  $\mathcal{O} \left( \frac{d}{\varepsilon} \right)$  neurons.  $\square$

The bound is not necessarily optimal, but it conveys a critical message about two-layer neural networks: the number of hidden neurons is only polynomial in  $d$ , instead of exponential eq. (35).

**Remark 2.** Several remarks are in place.

- *Why are multilayer neural networks preferred?* We have seen that to achieve the accuracy  $\varepsilon$  it requires  $\mathcal{O}(\varepsilon^{-d})$  hidden layers for one layer neural network, which is computational intractable when  $d$  is large. For the two-layer neural network, however, the numbers of hidden layer required are only linear or quadratic ( $\mathcal{O}\left(\frac{d^2}{\varepsilon^2}\right)$  for the first layer and  $\mathcal{O}\left(\frac{d}{\varepsilon}\right)$  for the second layer. In particular, if we can find the activation in theorem 3, we only need  $3d$  neurons in the first layer and  $6d + 3$  in the second layer. For example, for the two-dimensional problem we are considering, a two-layer neural network with hidden units 6 and 15 is sufficient to represent any continuous function. It is an astonishing fact. However, since these activation functions are hard to find, and also we need to consider the optimization algorithm, in practice, we may use simpler activation functions such as sigmoid,  $\tanh$  or ReLU. Besides, increasing the number of layers may help; in some sense, we are approximating the “oracle” activation function by another neural network. Another demonstration of the superior of multilayer neuron networks over a single layer neuron network is that the latter has a lower bound regarding approximation, see [27, 30] for details.
- *Approximation and Optimization.* One advantage of neural networks is that an optimal two-layer neural network (in Kolmogorov superposition theorem) is able to represent the function exactly. Linear basis functions in finite element method, radial basis functions in the mesh-less methods and so on do not have this property. However, we need to be careful when using neural networks to approximate a function. The resulting optimization problem is known to be difficult and may have many nonlocal minimums. Researchers have designed many architectures such as convolutional neural network, ResNet, DenseNet, etc. in the hope that the optimization will be easier without compromising the approximation ability too much. An active research area currently is the neural architecture search (NAS) which aims to find a good architecture for particular problems automatically. Those efforts can be viewed as striking a balance between approximation and optimization.

#### 4.2. Types of Error and Convergence

In this section, we derive an error bound for the amplitude of the calibrated characteristic function (CCF) and that of the empirical characteristic function. That is equivalent to consider the real part of those functions. Since we are only concerned with the error due to the neural network approximation, we might as well assume the empirical characteristic exponent in eq. (29) is exact, i.e.,  $I_E(\xi) = I(\xi)$ . We define the mismatch function

$$g(\xi) = -\frac{1}{2} \langle \xi, A^* \xi \rangle + \sum_{k=1}^{n_q^2} (\cos \langle \xi, \mathbf{x}_k \rangle - 1) \nu_{\mathbf{w}^*}(\mathbf{x}_k) w_k - \left( -\frac{1}{2} \langle \xi, A \xi \rangle + \int_{\mathbb{R}^2} (\cos \langle \xi, \mathbf{x} \rangle - 1) \nu(\mathbf{x}) d\mathbf{x} \right) \quad (51)$$

We make the following assumptions

**Assumption 1.** The Lévy measure  $\nu(\mathbf{x})$  is continuous and

$$\|\nu(\mathbf{x})\|_1 = \int_{\mathbb{R}^2} |\nu(\mathbf{x})| d\mathbf{x} < \infty \quad \|\nu(\mathbf{x})\|_\infty < \infty \quad \|\nu(\mathbf{x})\|_* = \int_{\mathbb{R}^2} |\nu(\mathbf{x})| \|\mathbf{x}\mathbf{x}^T\|_2 d\mathbf{x} < \infty \quad (52)$$

**Assumption 2** (Optimization Error). Given the training points  $\{\xi_j\}_{j=1}^n$  in the frequency domain, the optimization of eq. (29) finds the parameters  $A^*$ ,  $\mathbf{w}^*$  that achieve a uniform upper bound  $\varepsilon_1$  satisfying for all  $j = 1, 2, \dots, n$

$$|g(\xi_j)| \leq \varepsilon_1 \quad j = 1, 2, \dots, n$$

**Assumption 3** (Location of Collocation Points). The collocation points  $\{\xi_j\}_{j=1}^n$  triangulated the domain  $\Omega$  into a partition  $\mathcal{T} = \{T_1, T_2, \dots, T_M\}$ , where  $T_i$  are triangles satisfying

$$\cup_{T \in \mathcal{T}} = \bar{\Omega} \quad T_i^\circ \cap T_j^\circ = \emptyset, i \neq j \quad (53)$$

Define  $h_T = \text{Area}(T)^{\frac{1}{2}}$  and  $\mathcal{T}$  is quasi-uniform in the sense [33]

$$\frac{\max_{T \in \mathcal{T}} \text{Area}(T)}{\min_{T \in \mathcal{T}} \text{Area}(T)} \leq \rho \quad (54)$$

In addition, define  $h = \max_{T \in \mathcal{T}} h_T$

**Remark 3.** Figure 1 example of the triangulation for  $[0, 1]^2$  that satisfies Assumption 3. It is not hard to see under this assumption, for sufficiently large  $n$ ,  $h \simeq \frac{1}{\sqrt{n}}$ . This assumption is very common in the finite element methods [34].

**Assumption 4** (Boundedness of Neural Network Approximations). There exists a constant  $c$  depending on  $\Omega$ , independent of the collocation points  $\{\xi\}_{j=1}^N$  and  $N$ , such that the neural network approximation  $\nu_{\mathbf{w}^*}(\mathbf{x})$  to  $\nu(\mathbf{x})$  satisfies

$$\|\nu_{\mathbf{w}^*}(\mathbf{x})\|_\infty \leq c \|\nu(\mathbf{x})\|_\infty \quad (55)$$

It may seem that Assumption 4 is not natural compared to the other three assumptions. However, this assumption is indeed required for any successful neural network approximation. Suppose that there exists a sequence of weights  $\mathbf{w}_n^*$  and collocation points set that  $\|\nu_{\mathbf{w}_n^*}(\mathbf{x}_n)\|_\infty \rightarrow \infty$ ,  $n \rightarrow \infty$ , it indicates that the neural architecture design or the optimization is not successful. Any reasonable procedure should yield a solution  $\nu_{\mathbf{w}^*}(\mathbf{x})$  that does not deviate too much from  $\nu(\mathbf{x})$ .

We can now prove the following theorem

**Theorem 5.** Assume that the above assumptions are fulfilled. Suppose the numerical quadrature is defined for  $\{\mathbf{x} : |\mathbf{x}| \leq R\}$ . Let  $\xi$  be any point in the convex hull of  $\{\xi_j\}_{j=1}^n$ , we have

$$|g(\xi)| \lesssim \varepsilon_1 + (\varepsilon_1 + \|\nu(\mathbf{x})\|_\infty + \|\nu(\mathbf{x})\|_1 + \|\nu(\mathbf{x})\|_*)h^2 \quad (56)$$

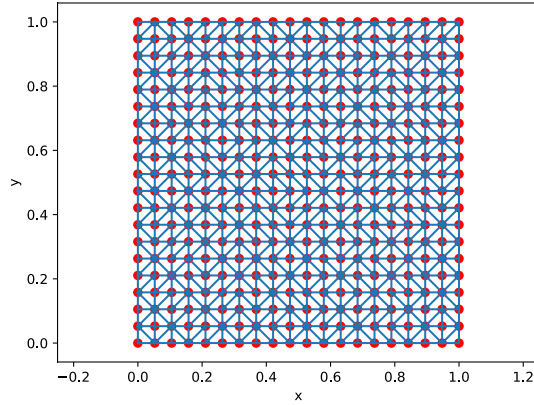


Figure 1: Example of the triangulation for  $[0, 1]^2$  that satisfies Assumption 3.

*Proof.* Since  $\xi$  is in the convex hull of  $\{\xi_j\}_{j=1}^n$ , it must lie on the boundary or inside some triangle  $T \in \mathcal{T}$  according to Assumption 3. Suppose the vertices of  $T$  are  $\xi_1, \xi_2, \xi_3$ , and  $\xi$  can be written as

$$\xi = \sum_{i=1}^3 \lambda_i \xi_i, \quad \sum_{i=1}^3 \lambda_i = 1, \quad \lambda_i \geq 0 \quad (57)$$

Note the gradient and Hessian of  $g(\xi)$  exist

$$\nabla g(\xi) = - (A^* - A)\xi - \sum_{k=1}^{n_q^2} \sin \langle \xi, \mathbf{x}_k \rangle w_k \nu_{\mathbf{w}^*}(\mathbf{x}_k) \mathbf{x}_k + \int_{\mathbb{R}^2} \sin \langle \xi, \mathbf{x} \rangle \mathbf{x} \nu(\mathbf{x}) d\mathbf{x} \quad (58)$$

$$\nabla^2 g(\xi) = - (A^* - A) - \sum_{k=1}^{n_q^2} \cos \langle \xi, \mathbf{x}_k \rangle w_k \nu_{\mathbf{w}^*}(\mathbf{x}_k) \mathbf{x}_k \mathbf{x}_k^T + \int_{\mathbb{R}^2} \cos \langle \xi, \mathbf{x} \rangle \nu(\mathbf{x}) \mathbf{x} \mathbf{x}^T d\mathbf{x} \quad (59)$$

we can revoke the multivariate Taylor's formula

$$\begin{aligned}
g(\xi_1) &= g(\xi) + \nabla g(\xi) \cdot (\xi_1 - \xi) + \sum_{|\beta|=2} (\xi_1 - \xi)^\beta \int_0^1 (1-t) D^\beta g(\xi + t(\xi_1 - \xi)) dt \\
g(\xi_2) &= g(\xi) + \nabla g(\xi) \cdot (\xi_2 - \xi) + \sum_{|\beta|=2} (\xi_2 - \xi)^\beta \int_0^1 (1-t) D^\beta g(\xi + t(\xi_2 - \xi)) dt \\
g(\xi_3) &= g(\xi) + \nabla g(\xi) \cdot (\xi_3 - \xi) + \sum_{|\beta|=2} (\xi_3 - \xi)^\beta \int_0^1 (1-t) D^\beta g(\xi + t(\xi_3 - \xi)) dt
\end{aligned}$$

Therefore we have

$$\sum_{i=1}^3 \lambda_i g(\xi_i) = g(\xi) + \sum_{i=1}^3 \lambda_i \sum_{|\beta|=2} (\xi_i - \xi)^\beta \int_0^1 (1-t) D^\beta g(\xi + t(\xi_i - \xi)) dt$$

Thus

$$|g(\xi)| \lesssim \sum_{i=1}^3 \lambda_i |g(\xi_i)| + \|\nabla^2 g\|_2 h^2 \leq \varepsilon_1 + \|\nabla^2 g\|_2 h^2$$

We now derive a bound for  $\|\nabla^2 g\|_2$ . Since we have  $|g(\xi)| \leq \varepsilon_1$  at collocation points, we have

$$\begin{aligned}
\left| \frac{1}{2} \langle \xi, (A - A^*) \xi \rangle \right| &\leq \varepsilon_1 + \sum_{k=1}^{n_q^2} (1 - \cos \langle \xi, \mathbf{x}_k \rangle) |\nu_{\mathbf{w}^*}(\mathbf{x}_k)| w_k + \int_{\mathbb{R}^2} (1 - \cos \langle \xi, \mathbf{x} \rangle) |\nu(\mathbf{x})| d\mathbf{x} \\
&\lesssim \varepsilon_1 + \|\nu(\mathbf{x})\|_\infty + \|\nu(\mathbf{x})\|_1
\end{aligned} \tag{60}$$

We have shown that eq. (60) implies that

$$\|A - A^*\|_2 \lesssim \varepsilon_1 + \|\nu(\mathbf{x})\|_\infty + \|\nu(\mathbf{x})\|_1 \tag{61}$$

therefore we have

$$\left| -(A^* - A) - \sum_{k=1}^{n_q^2} \cos \langle \xi, \mathbf{x}_k \rangle w_k \nu_{\mathbf{w}^*}(\mathbf{x}_k) \mathbf{x}_k \mathbf{x}_k^T + \int_{\mathbb{R}^2} \cos \langle \xi, \mathbf{x} \rangle \nu(\mathbf{x}) \mathbf{x} \mathbf{x}^T d\mathbf{x} \right| \tag{62}$$

$$\lesssim \|A^* - A\| + R^2 \|\nu(\mathbf{x})\|_\infty \sum_{k=1}^{n_q^2} w_k + \int_{\mathbb{R}^2} |\nu(\mathbf{x})| \|\mathbf{x} \mathbf{x}^T\|_2 d\mathbf{x} \tag{63}$$

$$\lesssim \varepsilon_1 + \|\nu(\mathbf{x})\|_\infty + \|\nu(\mathbf{x})\|_1 + R^4 \|\nu(\mathbf{x})\|_\infty + \|\nu(\mathbf{x})\|_* \tag{64}$$

$$\lesssim \varepsilon_1 + \|\nu(\mathbf{x})\|_\infty + \|\nu(\mathbf{x})\|_1 + \|\nu(\mathbf{x})\|_* \tag{65}$$

Therefore

$$\|\nabla^2 g\|_2 \lesssim \varepsilon_1 + \|\nu(\mathbf{x})\|_\infty + \|\nu(\mathbf{x})\|_1 + \|\nu(\mathbf{x})\|_* \tag{66}$$

□

**Remark 4.** We need to make a vital remark here. The error bound tells us that if the model is correct, there are two error sources for the current algorithm: the *optimization error*  $\varepsilon_1$ , which depends on the ability to find the minimum the neural network optimizer. Note it is observed widely in the literature that a neural network approximation might lead to a non-convex optimization problem which may assume many local minimums. It is an NP-hard problem if no other information is available [35]. Suggestions on reducing this error include using Stochastic Gradient Descent to escape the saddle points, training for a longer time, designing a more favorable neural network architecture, etc.

The other error – the *consistency error*,  $(\varepsilon_1 + \|\nu(\mathbf{x})\|_\infty + \|\nu(\mathbf{x})\|_1 + \|\nu(\mathbf{x})\|_*)h^2$  – comes from the number of training data. One remarkable observation is that we expect a linear reduction in the point-wise error (since  $h^2 \simeq \frac{1}{n}$ ) as we increase the number of training data. Note the constant  $(\varepsilon_1 + \|\nu(\mathbf{x})\|_\infty + \|\nu(\mathbf{x})\|_1 + \|\nu(\mathbf{x})\|_*)$  also depends on the optimization error.

The discussion above clearly sketches out the convergence behavior as we increase the number of training data. When  $n$  is small, the consistency error dominates, and therefore we expect to see a linear reduction in the error as  $n$  increases; at some point, due to the small consistency error and larger optimization error due to the larger training samples, the optimization error will eventually dominate. If there is no essential change in the optimizer, we expect the error to remain at the same level or even grows larger at this stage. Later, we will show the astonishing coincidence between the numerical results and the theoretical prediction.

## 5. Numerical Experiments

In this section, we analyze the methods proposed in this paper and consider an application for the stock markets. The experiments are carried out in  $\mathbb{R}^2$  but can be easily generalized to higher dimensions (possible challenges are the curse of dimensionalities for the quadrature rules). We implemented the algorithms using `TensorFlow.jl`, a Julia wrapper for `TensorFlow`.

### 5.1. $\alpha$ -stable distribution

The calibration problem is the inverse of the  $\alpha$ -stable distribution with characteristic exponent eq. (12). We consider a special case where the explicit characteristic exponents are available: symmetric  $\alpha$ -stable distribution, with characteristic exponent

$$I(\xi) = -|\xi|^\alpha \tag{67}$$

the corresponding  $\Gamma$  in eq. (12) will be constant on  $S^d$ . We use a two-layer neural network with hidden sizes 20. The activation function is `tanh` since it is smooth. We use `AdamOptimizer` with default parameters and train the model for 5000 iterations. The initial guess for  $\alpha$  is 1 but can be selected randomly from  $(0, 2]$ . Figure 2 shows the convergence of the trained  $\alpha$  as well as the value of the loss function as the training proceeds. We can see that the  $\alpha$  index converges to the exact value very accurately. The loss does not necessarily

go to zero due to a local minimum, the approximation degree of the neural network as well as the discretization error from the quadrature rule. Overall, the results are accurate enough for many practical uses.

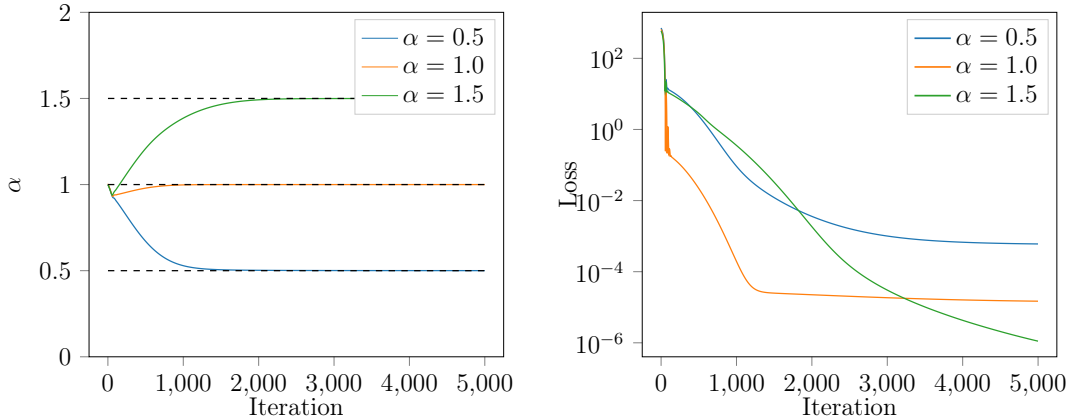


Figure 2: Calibration of the stable index in the  $\alpha$ -stable distribution. Left: Parameter evolution with respect to iterations. The legend shows the true parameters. Right: The loss function for each case. A two-layer neural network with hidden sizes  $n_h = 20$  is used.

### 5.2. Lévy Process

In this section, we consider calibrating the Lévy measure in eq. (28). Since for small  $n$ , we may encounter the problem of overfitting, it is not advisable to use the loss function as an error metric. Instead, we measure the error by the root mean squared error, given by

$$RMSE(\mathbf{w}, A) = \sum_{j=1}^{1000} \left( -\frac{1}{2} \langle \xi'_j, A \xi'_j \rangle + \sum_{k=1}^{n_q^2} (\cos \langle \xi'_j, \mathbf{x}_k \rangle - 1) \nu_{\mathbf{w}}(\mathbf{x}_k) w_k - \Re I_E(\xi'_j) \right)^2 \quad (68)$$

where  $\{\xi'_j\}_{j=1}^{1000}$  are 1000 random samples from the frequency domain. We considered dense neural networks with various number of layers, hidden sizes. Also we vary the number of quadrature points  $n_q^2$  and the number of training points. The neural network is trained using `AdamOptimizer` and for 50000 iterations.

Figure 3 shows the convergence plot for calibration the non-parametric Lévy process. As the number of training point increases, the mean squared error tends to decrease in different settings until around  $n = 100$ . They all achieve or surpass the predicted convergence rate  $\mathcal{O}(n^{-1}) = \mathcal{O}(h^2)$ . For  $n \leq 100$ , the consistency error dominants and therefore we can reduce the error by increasing the training points. However, after  $n \geq 100$ , either discretization error or optimization error dominates. In consideration of the highly accurate quadrature rules we have used, we can conclude that the optimization will be the bottleneck. We demonstrate increase the quadrature rules from  $n_q = 20$  to  $n_q = 30$  but can see no substantial improvement. In that case, the optimizer might get stuck at a local minimum, or it requires more training time. The rate of convergence is computed using the first 4 data points.

Figure 4 shows the root mean squared error for different  $n_q$ ,  $n_l$  and  $n_h$ . The neural network is trained using  $n = 1000$  sample points. As we can see the accuracy of the algorithm improves as we use a more accurate numerical quadrature rule (larger  $n_q$ ). It demonstrates the idea of discretization error. We also notice that for  $n_l = 10$ ,  $n_h = 128$ , the error does not decrease even if  $n_q$  increases. That is because in this case, the neural network is so large that 50000 iterations and  $n = 1000$  sample points are not sufficient for the optimizer to find an adequate (local) minimum. We also see that on average smaller  $n_l$  leads to smaller RMSE. That is because for our model two-layer neural network is sufficient to represent the Lévy measure and much easier to train than its counterparts.

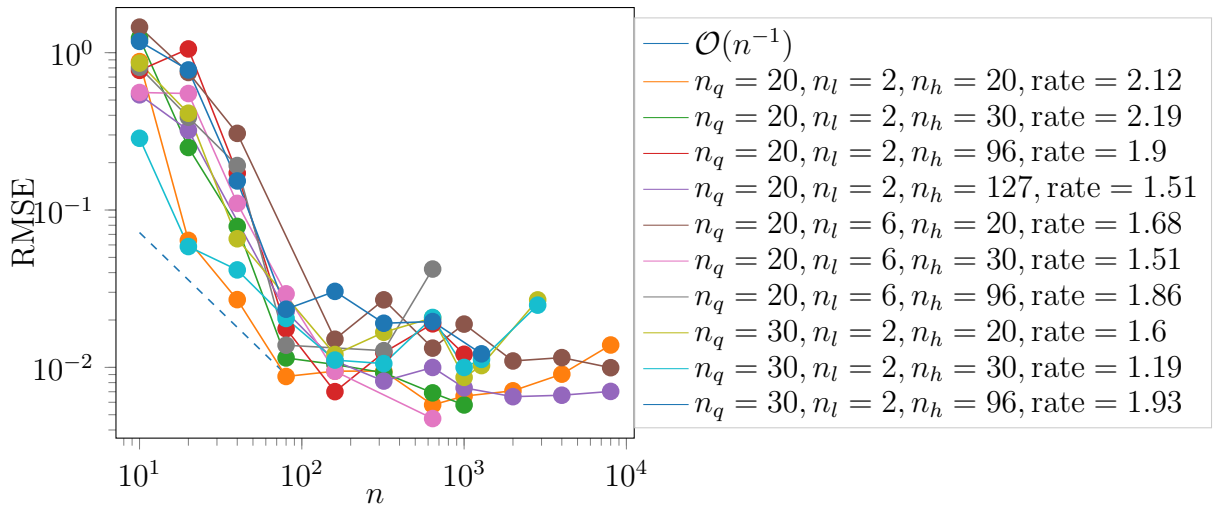


Figure 3: Convergence plot for calibration the non-parametric Lévy process. As the number of training point increases, the mean squared error tends to decrease in different settings until around  $n = 100$ . They all achieve or surpass the predicted convergence rate  $\mathcal{O}(n^{-1}) = \mathcal{O}(h^2)$ . For  $n \leq 100$ , the consistency error dominants and therefore we can reduce the error by increasing the training points. However, after  $n \geq 0$ , either discretization error or optimization error dominates. In consideration of the highly accurate quadrature rules we have used, we can conclude that the optimization will be the bottleneck. We demonstrate it numerically by increasing the quadrature rules from  $n_q = 20$  to  $n_q = 30$  but can see no substantial improvement. In that case, the optimizer might get stuck at a local minimum, or it requires more training time. The rate of convergence is computed using the first 4 data points.

### 5.3. Application to the Stock Market

We consider an application of the multivariate stable distribution for pairs of stocks. The data is from the daily adjusted-close price from 11/01/2008 to 11/01/2018. Figure 5 shows the log return of the apple stock during this period. We model the log return of pairs of stocks by the multivariate stable distribution. We investigate 12 stocks, which are from the technology sector (MSFT, AAPL, AMZN, GOOG), financial sector (JPM, C, WFC, CME) and energy sector (EOG, XOM, ESV, ENB). The neural network is a simple dense neural network with two hidden layers, and the hidden sizes are 20. We use `AdamOptimizer` for optimization, with default parameters and it was for 50000 iterations. Figure 6 shows the learnt  $\alpha$  for each pairs of stocks. The  $i$ -th row and  $j$ -th column denote the  $\alpha$  corresponding

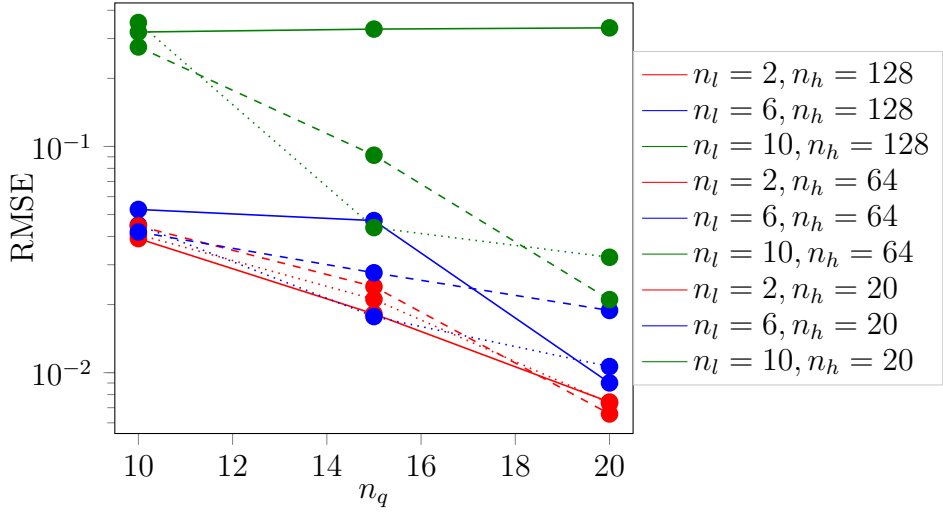


Figure 4: Root mean squared error for different  $n_q$ ,  $n_l$  and  $n_h$ . The neural network is trained using  $n = 1000$  sample points. As we can see the accuracy of the algorithm improves as we use a more accurate numerical quadrature rule (larger  $n_q$ ). It demonstrates the idea of discretization error. We also notice that for  $n_l = 10$ ,  $n_h = 128$ , the error does not decrease even if  $n_q$  increases. That is because in this case, the neural network is so large that 50000 iterations and  $n = 1000$  sample points are not sufficient for the optimizer to find an adequate (local) minimum. We also see that on average smaller  $n_l$  leads to smaller RMSE. That is because for our model two-layer neural network is sufficient to represent the Lévy measure and much easier to train than its counterparts.

to  $i$ -th stock as the first variable while the other as the second. We see a clear pattern for some stocks: for example, EOG has a smaller  $\alpha$  index with C and ESV.

$n_q$	$n$	$n_l$	$n_h$	$a$	$b$	$c$	RMSE	Time (sec)
30	1280	6	20	1.0215	0.9997	1.0184	0.0065	1607.46
20	640	2	20	0.9570	0.9883	0.9536	0.0058	1400.97
20	1000	2	32	0.9544	0.9909	0.9516	0.0058	1354.93
30	1000	6	32	1.0191	1.0014	1.0186	0.0050	1577.66
20	640	6	32	0.9462	0.9952	0.9442	0.0047	1588.72

Table 2: The best five experiment results for different  $n_q$ ,  $n$ ,  $n_l$ ,  $n_h$ . The true parameters are  $a = b = c = 1$ . We can see the winners usually do not have very complicated structures ( $n_h = 20$  or  $32$  while  $n_l = 2$  or  $6$ , they are the smallest parameters for  $n_h$ ,  $n_l$  for all our experiments), nor do they require large training samples. Almost everything boils down to the difficulty of optimization when a large neural network or large training samples are used. In addition, as we have discussed, a two-layer neural network is actually very powerful for low dimensional inputs. Adding more neurons or layers suffers from diminishing marginal benefits.

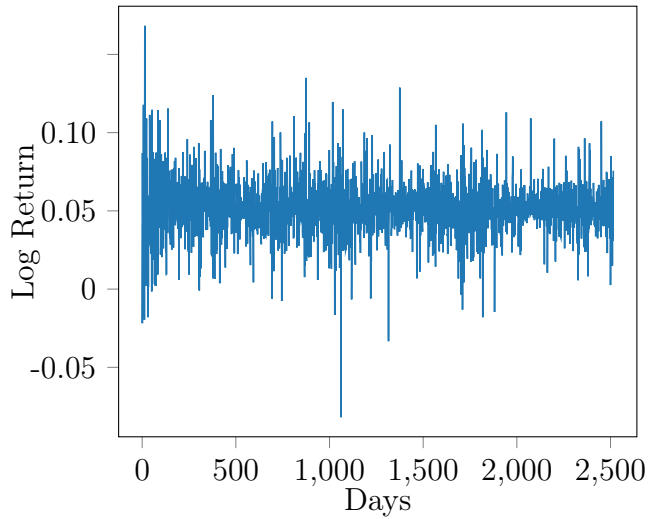


Figure 5: The log return of the stock AAPL from 11/01/2008 to 11/01/2018.

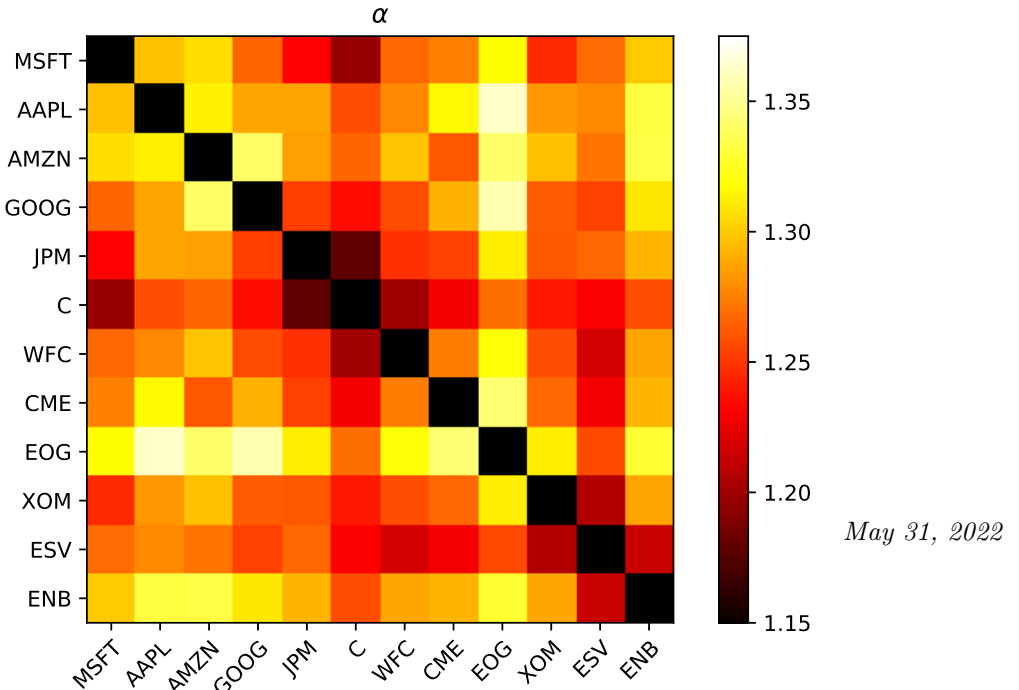


Figure 6:  $\alpha$  index computed from daily adjust-close prices. The  $i$ -th row and  $j$ -th column denotes the  $\alpha$  index for the  $i$ -th day with the  $j$ -th stock. The first variable will be the  $i$ -th row and the second variable will be the  $j$ -th column. We can observe that the  $\alpha$  index for

We show the histograms of these stocks the log returns in fig. 7. For comparison, we also include APPL vs. EOG data. Intuitively the histograms of C/EVS vs. EOG are much thinner than that of AAPL vs. EOG. Figures 8 to 10 show the calibrated characteristic functions and empirical characteristic functions for these stocks. Interestingly, the contour of the spectrum amplitudes for ESV/C vs. EOG is more like a rectangular, indicating a non-Gaussian distribution. The contour for APPL vs. EOG is more like an eclipse. The  $\alpha$  indexes we have learned well capture those distinguishing characteristics. A deeper investigation is required to reveal more facts underlying this result.

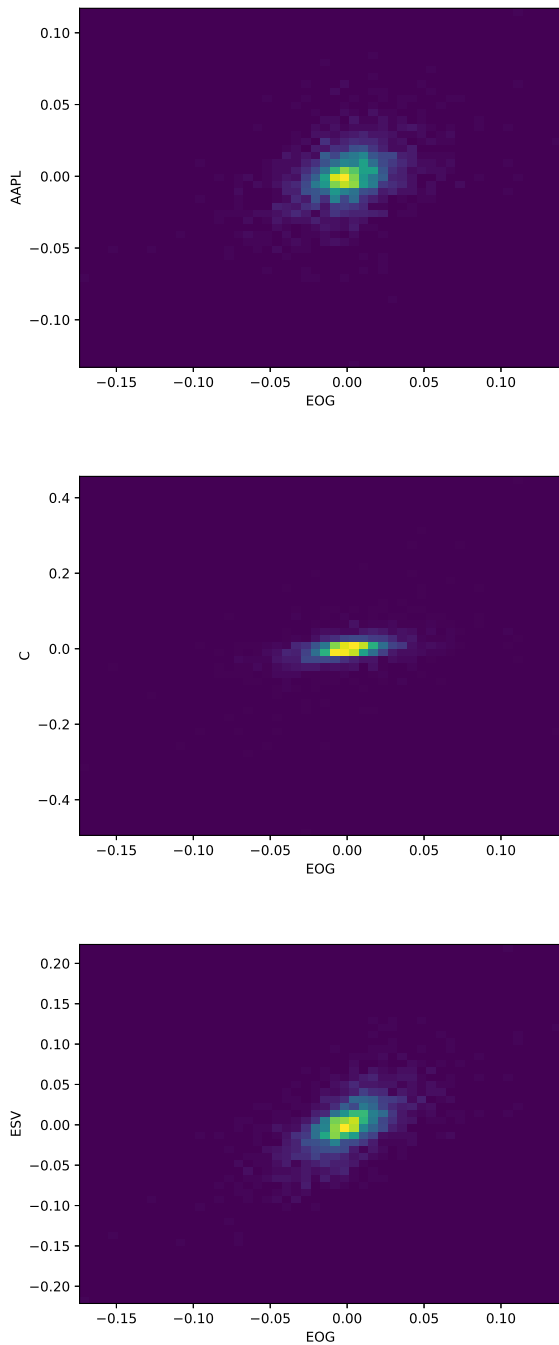


Figure 7: Histogram of the log return. Top: AAPL; Middle: C; Bottom: ESV. Intuitively the histograms of C/EVS vs. EOG are much thinner than that of AAPL vs. EOG.

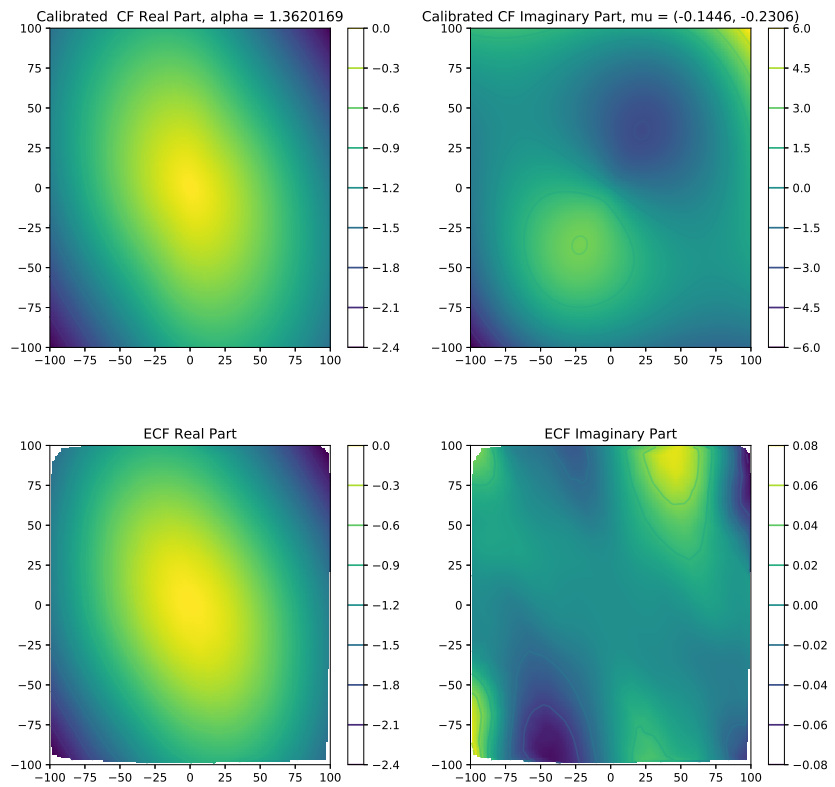


Figure 8: Calibrated characteristic exponents and empirical characteristic exponents for AAPL vs. EOG.

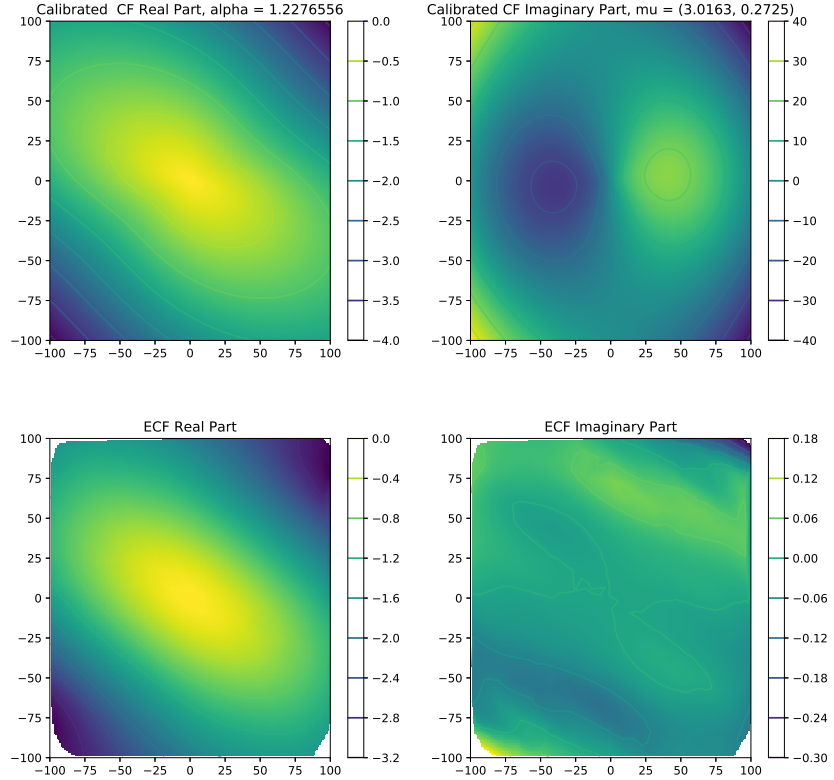


Figure 9: Calibrated characteristic exponents and empirical characteristic exponents for ESV vs. EOG.

## 6. Conclusion

We proposed a framework for calibration multivariate distribution derived from the Lévy process using machine learning techniques. We have used multilayer neural networks for approximating the nonparametric part of the distribution, i.e., the Lévy density function. For minimizing the loss function, we adopted the `AdamOptimizer` which proves useful in deep learning. For computing the gradients of the loss function, we chose the automatic differentiation. There are many problems to be further explored, such as the choice of the neural network architectures, the selection of optimizers, the role multilayer neural networks play over one or two layer neural networks, etc. Our premise is that more layers will make the required number of neurons for each layer smaller, even constant for three or more layers. However, we need to point out that more layers and more neurons per hidden layer will lead to the difficulty of optimization, which is a critical tradeoff we need to consider in practice. One of the significant findings for the paper is that we have given an explicit number of neurons required for each layer for a two-layer neural network with sigmoid activations functions if a certain accuracy is desired. Another finding is that the RMSE of the algorithm will decrease linearly in the number of training points, and one of our numerical examples demonstrated

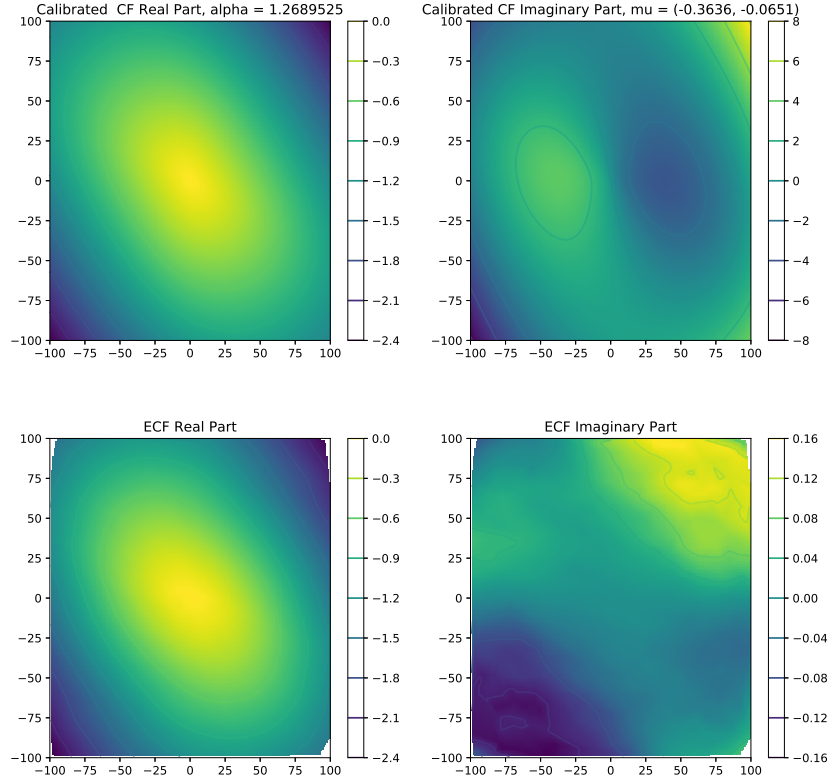


Figure 10: Calibrated characteristic exponents and empirical characteristic exponents for C vs. EOG.

the claim. We also considered an important application of the proposed algorithm to the stock markets, where we find some patterns in the  $\alpha$ -index for several stocks.

Despite the effectiveness of the proposed algorithm, there are still many problems to be solved in the further. One problem is a more comprehensive understanding of the neural network approximation and non-convex optimization. Even though the multilayer neural network and other architectures work so well in many applications, the mathematical theory is elusive. Another problem is that a general non-convex optimization problem is NP-hard. A single optimization execution does not guarantee the convergence to the global minimum. An efficient optimization algorithm and a convergence proof are desired from a theoretical aspect. However, we do not pursue this in the paper but merely assume the accuracy of the optimization. Finally, we have only considered the constant coefficients Lévy process. It would be more general to discuss the case where  $\xi$ ,  $A$  and  $\nu(y)$  may depend on time  $t$  and location  $\mathbf{x}$ .

We believe the techniques proposed in this paper will benefit other similar problems, i.e., the idea of nonlinear approximation by multilayer neural networks, gradient computation by the automatic differentiation, and the mix of the numerical discretization and the optimization technique. It opens the possibility of treating engineering problems from a fresh new perspective.

# Appendices

## A. Hilbert's 13-th Problem

Hilbert's 13-th problem was proposed as follows [36]:

Is the root of the equation

$$x^7 + ax^3 + bx^2 + cx + 1 = 0 \quad (69)$$

a superposition of continuous functions of two variables?

## B. Quadrature on a Disk

It is not easy to derive optimal cubature to achieve a given algebraic degree on a disk is not easy. The only known quadrature rules are for degree  $N = 3, 4, 6, 7, 10, 12, 18$ .

Another strategy is to use the tensor Gauss quadrature rules in the polar coordinates. The idea is to rewrite the integral for  $x^i y^j$  into

$$\iint_{x^2+y^2 \leq 1}^i y^j dx dy = \int_{-1}^1 |\rho| \rho^{i+j} d\rho \int_{-\frac{\pi}{2}}^{\frac{\pi}{2}} \cos^j \varphi \sin^j \varphi d\varphi \quad (70)$$

$$= \int_{-1}^1 |\rho| \rho^{i+j} d\rho \int_{-1}^1 (1-t^2)^{-1/2} (1-t^2)^{i/2} t^j dt \quad (71)$$

We then can apply Gauss-Chebyshev formula of the first kind for approximation

$$\int_{-1}^1 (1-t^2)^{-1/2} (1-t^2)^{i/2} t^j dt$$

with the weight function  $(1-t^2)^{-1/2}$ . And we build Gauss quadrature for the outer integration. Figure 11 shows an example of the quadrature nodes in the unit disk  $B_0(1)$  of order  $n_q = 20$ . We use the open source codes published on [37] for the implementation.

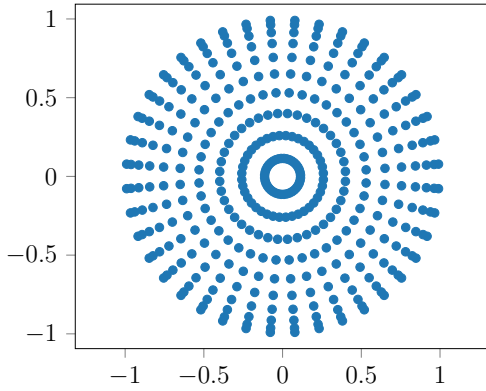


Figure 11: An example of the quadrature nodes in the unit disk  $B_0(1)$  of order 20. There are 400 nodes in total.

## References

### References

- [1] C. Menn and S. T. Rachev. Calibrated FFT-Based Density Approximations for  $\alpha$ -Stable Distributions. *Computational statistics & data analysis*, 50(8):1891–1904, 2006.
- [2] P. Tankov. Financial Modeling with Lévy Processes. 2010.
- [3] R. C. Merton. Option Pricing When Underlying Stock Returns Are Discontinuous. *Journal of financial economics*, 3(1-2):125–144, 1976.
- [4] S. G. Kou. A Jump-Diffusion Model for Option Pricing. *Management science*, 48(8):1086–1101, 2002.
- [5] D. B. Madan, P. P. Carr, and E. C. Chang. The Variance Gamma Process and Option Pricing. *Review of Finance*, 2(1):79–105, 1998.
- [6] P. Carr, H. Geman, D. B. Madan, and M. Yor. The Fine Structure of Asset Returns: An Empirical Investigation. *The Journal of Business*, 75(2):305–332, 2002.
- [7] N. Laskin. Principles of Fractional Quantum Mechanics. *arXiv preprint arXiv:1009.5533*, 2010.
- [8] M. Hasan and B. P. Mandal. Tunneling Time in Space Fractional Quantum Mechanics. *Physics Letters A*, 382(5):248–252, 2018.
- [9] P. Garbaczewski, J. R. Klauder, and R. Olkiewicz. Schrödinger Problem, Lévy Processes, and Noise in Relativistic Quantum Mechanics. *Physical Review E*, 51(5):4114, 1995.
- [10] N. Laskin. Fractional Quantum Mechanics and Lévy Path Integrals. *Physics Letters A*, 268(4-6):298–305, 2000.
- [11] M. Annunziato and H. Gottschalk. Calibration of Lévy Processes Using Optimal Control of Kolmogorov Equations with Periodic Boundary Conditions. *arXiv preprint arXiv:1506.08439*, 2015.
- [12] A. Krizhevsky, I. Sutskever, and G. E. Hinton. Imagenet Classification with Deep Convolutional Neural Networks. *Imagenet Classification with Deep Convolutional Neural Networks*, pages 1097–1105, 2012.
- [13] T. Young, D. Hazarika, S. Poria, and E. Cambria. Recent Trends in Deep Learning Based Natural Language Processing. *ieee Computational intelligence magazine*, 13(3):55–75, 2018.
- [14] D. Silver, J. Schrittwieser, K. Simonyan, I. Antonoglou, A. Huang, A. Guez, T. Hubert, L. Baker, M. Lai, A. Bolton, et al. Mastering the Game of Go Without Human Knowledge. *Nature*, 550(7676):354, 2017.
- [15] J. M. Zurada. *Introduction to artificial neural systems*, volume 8. West publishing company St. Paul, 1992.
- [16] A. G. Baydin, B. A. Pearlmutter, A. A. Radul, and J. M. Siskind. Automatic Differentiation in Machine Learning: A Survey. *Journal of Machine Learning Research*, 18:1–43, 2018.
- [17] S. E. Fahlman et al. An Empirical Study of Learning Speed in Back-Propagation Networks. 1988.
- [18] V. Kurkova. Kolmogorov’s Theorem and Multilayer Neural Networks. *Neural networks*, 5(3):501–506, 1992.

- [19] R. Battini. A Multilayer Neural Network with Piecewise-Linear Structure and Back-Propagation Learning. *IEEE Transactions on Neural Networks*, 2(3):395–403, 1991.
- [20] Y. LeCun, Y. Bengio, and G. Hinton. Deep Learning. *nature*, 521(7553):436, 2015.
- [21] J. Yu. Empirical Characteristic Function Estimation and Its Applications. *Econometric reviews*, 23(2):93–123, 2004.
- [22] J. P. Nolan. An Overview of Multivariate Stable Distributions. *Online: <http://academic2.american.edu/jpnolan/stable/overview.pdf>*, 2008.
- [23] S. Borak, W. Härdle, and R. Weron. Stable Distributions. *Stable Distributions*, pages 21–44. Springer, 2005.
- [24] S. Mitnik, T. Doganoglu, and D. Chenyao. Computing the Probability Density Function of the Stable Paretian Distribution. *Mathematical and Computer Modelling*, 29(10-12):235–240, 1999.
- [25] J. P. Nolan. Numerical Calculation of Stable Densities and Distribution Functions. *Communications in statistics. Stochastic models*, 13(4):759–774, 1997.
- [26] H. Ogata. Estimation for Multivariate Stable Distributions with Generalized Empirical Likelihood. *Journal of Econometrics*, 172(2):248–254, 2013.
- [27] A. Pinkus. Approximation Theory of the MLP Model in Neural Networks. *Acta numerica*, 8:143–195, 1999.
- [28] P. Tankov. *Financial modelling with jump processes*, volume 2. CRC press, 2003.
- [29] G. Deelstra and A. Petkovic. How They Can Jump Together: Multivariate Lévy Processes and Option Pricing. *Belgian Actuarial Bulletin*, 9(1):29–42, 2010.
- [30] H. N. Mhaskar. Neural Networks for Optimal Approximation of Smooth and Analytic Functions. *Neural computation*, 8(1):164–177, 1996.
- [31] G. G. Lorentz, M. von Golitschek, and Y. Makovoz. *Constructive approximation: advanced problems*, volume 304. Springer Berlin, 1996.
- [32] V. Maiorov and A. Pinkus. Lower Bounds for Approximation By MLP Neural Networks. *Neurocomputing*, 25(1-3):81–91, 1999.
- [33] Ch2FEM.pdf. <https://www.math.uci.edu/~chenlong/226/Ch2FEM.pdf>. (Accessed on 12/11/2018).
- [34] I. Babuška and M. Suri. The  $H_p$  Version of the Finite Element Method with Quasiuniform Meshes. *ESAIM: Mathematical Modelling and Numerical Analysis*, 21(2):199–238, 1987.
- [35] A. Blum and R. L. Rivest. Training A 3-Node Neural Network Is NP-Complete. Training A 3-Node Neural Network Is NP-Complete, pages 494–501, 1989.
- [36] G. G. Lorentz. The 13th Problem of Hilbert. The 13th Problem of Hilbert, volume 28, pages 419–430. American Mathematical Society, 1976.
- [37] Cubature Formulas for the Unit Disk. <http://www.holoborodko.com/pavel/numerical-methods/numerical-integration/cubature-formulas-for-the-unit-disk/>. (Accessed on 12/15/2018).